3. E. D. Lyumkis, B. Ya. Martuzan, and E. N. Martuzane, "Interaction of fluxes caused by thermocapillary convection and rotation during zone melting and their influence on the propagation of impurities," Technological Experiments in Weightlessness [in Russian], Sverdlovsk (1983).
4. N. Kobayashi, "Power required to form a floating zone and zone shape," J. Crystal Growth, 43, 417 (1978).
5. D. K. Donald, "Thermal mode under vacuum melting conditions," Rev. Sci. Instrum., No. 7 (1961).
6. A. A. Samarskii, Introduction into the Theory of Difference Schemes [in Russian], Nauka, Moscow (1971).

STEADY-STATE CONFIGURATIONS OF THE DEFORMATION REGION AND THE FORCE BALANCE IN THE DRAWING OF AN OPTICAL FIBER

V. N. Vasil'ev and V. D. Naumchik

UDC 532.522 + 681.7.068.4

Fiber light guides are thin glass fibers formed from a liquid mass drawn through a die or pulled from a cylindrical semifinished product as a result of its symmetrical local heating to about 2000°C. Passing through air, the quartz glass melt forms a liquid stream with a free surface whose form is determined by the equilibrium between the forces of internal friction, surface tension, gravity, friction against the air, the force of acceleration on the glass, and the shearing force. The stream cools as it descends and, after application of the first polymer coating, the cold fiber enters a rotating drum. The drum maintains tension in the stream, forcing it to become thinner as cooling proceeds. The behavior of the molten stream of quartz glass can be examined on the basis of the gasdynamic equations of an incompressible Newtonian fluid and the energy equations, since the equation of motion contains the absolute viscosity – which is a function of temperature. Recent experimental findings show that shear flow occurs during the drawing of optical fibers [1]. Until now, there has been no reliable theory for calculation of the two-dimensional distribution of temperature and velocity in a jet of a high-viscosity liquid with a free surface. Thus, it is usually the practice to make several assumptions (examined in more detail in [2]) which make it possible to reduce the problem to a unidimensional problem. However, no detailed analysis of the drawing of optical fibers has been made even within the framework of unidimensional models. Here, the approaches have been either to solve only the hydrodynamic problem and assume that the viscosity distribution along the deformation is simply prescribed or to introduce an excessively simplified energy equation which does not adequately describe the process of heat transfer during fiber drawing.

Here, we examine the main results of a study of the formation of optical fibers obtained on the basis of a quasiunidimensional mathematical model whose basis principles were described in [3]. We will also analyze the balance of the forces acting in the deformation region during the formation of a fiber by the bead method.

1. The process of the formation of an optical fiber is examined in the simple uniaxial tension of a Newtonian fluid with variable viscosity determined by the temperature distribution. The temperature distribution is found from the energy equation. In formulating the system of equations describing the dynamics of fiber drawing, it was assumed that except for viscosity, the physical properties of the liquid are constant, the liquid is isotropic, and its motion is axisymmetric.

The equations of continuity

$$-\frac{\partial R}{\partial \tau} = v\frac{\partial R}{\partial x} + \frac{R}{2}\frac{\partial v}{\partial x}; \qquad (1.1)$$

Leningrad. Translated from Zhurnal Prikladnoi Mekhaniki i Tekhnicheskoi Fiziki, No. 2, pp. 77-84, March-April, 1988. Original article submitted January 4, 1987.

0021-8944/88/2902-0231$12.50

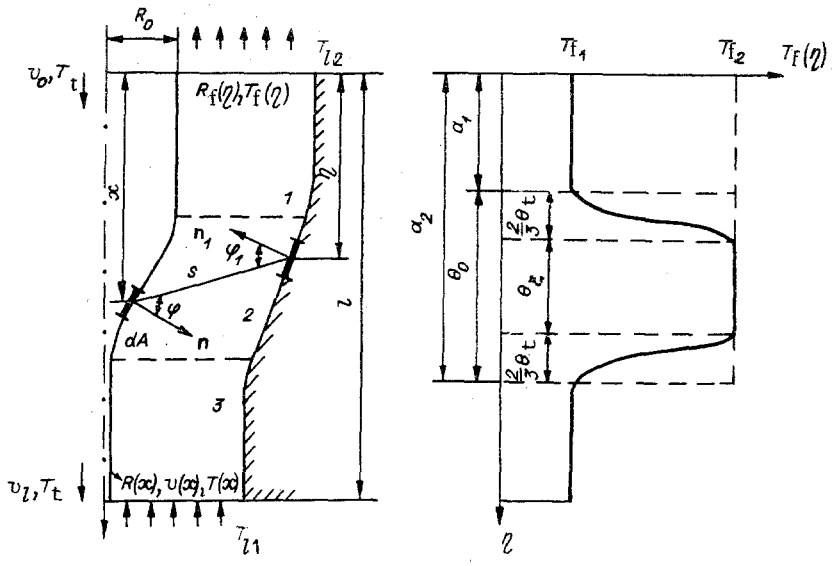

Fig. 1

of motion

$$\rho\left(\frac{\partial v}{\partial \tau}+v\frac{\partial v}{\partial x}\right)=\frac{1}{R^2}\frac{\partial}{\partial x}\left(3\mu R^2\frac{\partial v}{\partial x}\right)+g\rho+\frac{1}{R^2}\frac{\partial \sigma R^2 H}{\partial x} \tag{1.2}$$

and energy for the heating of the semifinished product in the furnace

$$c\rho\left(\frac{\partial T}{\partial \tau}+v\frac{\partial T}{\partial x}\right)=\frac{1}{R^2}\frac{\partial}{\partial x}\left(R^2\lambda_{ef}\frac{\partial T}{\partial x}\right)-\frac{2(1+R'^2)^{1/2}h}{R}(T-T_l)+$$
$$+\frac{4n_c^2\sigma_0(1+R'^2)^{1/2}}{R}\int_0^l\frac{R_f(\eta)\left[1+R_f'^2(\eta)\right]^{1/2}\left[\varepsilon_f\beta T_f^4(\eta)-\varepsilon T^4\right]}{(\eta-x)^2+[R_f(\eta)-R]^2}\cos\varphi\cos\varphi_1 d\eta \tag{1.3}$$

were obtained from the laws of conservation of mass, momentum, and energy [3]. Here, R is the form of the surface of the stream; v, longitudinal component of the motion of the glass; τ, time; x, longitudinal coordinate; g, acceleration due to gravity; μ, absolute viscosity; σ, surface tension; c, specific heat; ρ, density; T, temperature; σ_0, Stefan–Boltzmann constant; ϵ and ϵ_p, integral emittances of the stream surface and furnace; β, absorption coefficient of the glass; $\beta = 1 - r$; r, coefficient of reflection from the stream surface, calculated from the Fresnel formulas; n_c, refractive index of the gas blown through the furnace; T_l, a function describing the distribution of the temperature of the gas along the theoretical region; R_f, a function describing the form of the generatrix of the surface of the heating element; h, local value of the coefficient of external heat transfer; T_f, temperature distribution along the surface of the heating element; H, mean curvature of the stream surface [2]:

$$H=\frac{1+R'^2-RR''}{2R(1+R'^2)^{3/2}},\quad \cos\varphi_1=\frac{1}{s(1+R_p'^2)^{1/2}}\left[R_f-R-|R_f'|(x-\eta)\right],$$
$$\cos\varphi=\frac{1}{s(1+R'^2)^{1/2}}\left[R_f-R-|R'|(x-\eta)\right],\quad s^2=(\eta-x)^2+[R_f(\eta)-R]^2,$$
$$R'=\frac{\partial R}{\partial x},\quad R''=\frac{\partial^2 R}{\partial x^2},\quad R_f'=\frac{dR_f}{d\eta}.$$

The last term in the right side of the energy equation characterizes the flow of radiant energy, which decreases from the surface of the heating element to the surface of an elementary area dA in the section x. The quantity λ_{ef} is present due to the fact that quartz glass melt is a translucent medium, and energy is transferred by conduction and radiation simultaneously. Estimates show that the approximation of an optically thick layer is not satisfied in the drawing of light guides. Rigorous solution of the problem of the simultaneous transfer of heat by radiation and convection entails serious mathematical difficulties because the

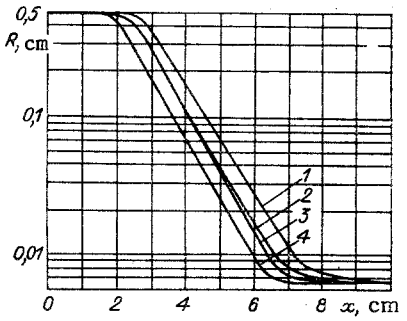

Fig. 2

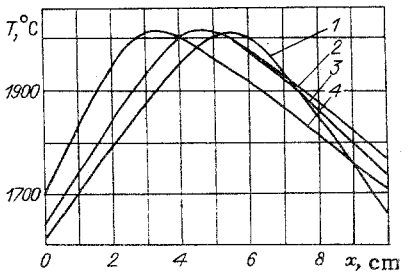

Fig. 3

energy and radiative transport equations are coupled; the radiation equation contains temperature, while the energy equation contains the density of the resulting radiant flux. Thus, to simplify the problem, it is best to approximate radiative heat transfer an analogy with the Fourier law and to find the coefficient of radiative heat transfer from the solution of the radiative transport equation, assuming that the temperature distribution and the form of the theoretical region are given. The last limitation, i.e. assigning the temperature distribution and the form of the theoretical region, is immaterial because the author of [3] has developed an algorithm to find the steady-state solution of system (1.1-1.3) based on the establishment method which makes it possible to correct the radiative heat-transfer parameters on the basis of another algorithm [4] as the iterations converge with respect to time.

Let us examine the calculation of the local coefficient of external heat transfer and the temperature of the gas blown through the heating zone. In calculating h and T_ℓ, we made the following assumptions:

1) estimates of the thickness of the boundary layer show that it does not completely fill the cross section of the channel. Thus, heat transfer can be examined independently for each wall;

2) since mixed convection takes place in the channel, the local value of the Nusselt number was found from the relation [5] $\mathrm{Nu}_x^3 = \mathrm{Nu}_{xc}^3 + \mathrm{Nu}_{x\,l}^3$. It was assumed that mixed convection occurs from a vertical cylinder on section 1 (Fig. 1), from a vertical cone on section 2, and, on section 3, from a thin vertical fiber in a longitudinal air flow and from the surface of the furnace – regarded as a vertical plate; the local value of the Nusselt number with natural convection Nu_{xn} and forced convection Nu_{xf} was found from the corresponding relations given in [6-8];

3) it was assumed that the temperature of the gas along the channel changes linearly from the temperature $T_{\ell 1}$ at the inlet to $T_{\ell 2}$ at the outlet; $T_l = (T_{l1} - T_{l2})x/l + T_{l2}$;

4) estimates show that the pressure gradient in the channel is much less than unity, so the temperature distribution in the channel can be found from the mass conservation law with allowance for thermal expansion of the gas, i.e. $v_g(x) = \frac{\rho_{gl} v_{gl}}{\rho_{g(x)}} \frac{\bar{R}_f^2 - R_l^2}{\bar{R}_f^2 - R^2(x)}$, where $\bar{R}_f = \frac{1}{l}\int_0^l R_f dx$ is the mean radius of the inside surface of the heating element; ρ_g is the density of the gas; v_g is the velocity of the gas; the subscript ℓ refers to parameters at the inlet of the channel.

On the basis of the law of energy conservation, the change in the internal energy of the gas is equal to the amount of heat supplied by the side walls of the channel, i.e.

$$\rho_{gl} c_{pl} v_f (\bar{R}_f^2 - R_l^2)(T_{l2} - T_{l1}) = 2\int_0^l h(T - T_l) R (1 + R'^2)^{1/2} dx + 2\bar{R}_f \int_0^l h_f (T_f - T_l) dx. \quad (1.4)$$

Inserting the relation $T_\ell(x)$ into (1.4) and solving the resulting equation for $T_{\ell 2}$ we obtain

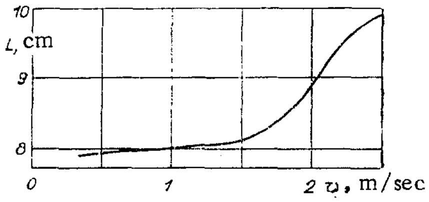

Fig. 4

$$T_{l2} = \frac{\frac{1}{2} T_{l1} \rho_{gl} c_{pl} v_{gl} (\bar{R}_f^2 - R_l^2) + \int_0^l \left\{ h\left(T - \frac{T_{l1}}{l} x\right) R (1+R'^2)^{1/2} + h_f \bar{R}_f \left(T_f - \frac{T_{l1}}{l} x\right)\right\} dx}{\frac{1}{2} \rho_{gl} c_{pl} v_{gl} (\bar{R}_f^2 - R_f^2) + \int_0^l \left(1 - \frac{x}{l}\right)\left[hR(1+R'^2)^{1/2} + h_f \bar{R}_f\right] dx}. \tag{1.5}$$

The temperature at the outlet of the channel is calculated by an iterative procedure. We assign a certain initial approximation of the temperature $T_{\ell 2}$, we calculate $T_\ell(x)$, $v_g(x)$, and Nu_x and we use (1.5) to refine the value of $T_{\ell 2}$. The iteration is ended when $|T_{l1}^i - T_{l1}^{i-1}| < \Delta$ (i is the number of the iteration and Δ is the accuracy of the computations). In Eqs. (1.4) and (1.5), h_f is the local value of the coefficient of external heat transfer from the surface of the furnace and $c_{p\ell}$ is the isobaric specific heat of the gas at the channel inlet.

As the first step in studying the formation of optical fibers, the author of [3] developed an algorithm for numerically solving the system of governing equations (1.1)-(1.3) in order to find the velocity and temperature distributions and the form of the deformation region in the steady state $(\partial T/\partial \tau = \partial v/\partial \tau = \partial R/\partial \tau = 0)$ with the following boundary conditions: $v = v_0$, $T = T_t$, $R = R_0$ at $x = 0$, $v = v_l$, $T = T_t$ at $x = \ell$, where v_0 is the rate of feed of the semifinished product into the heating zone; v_ℓ is the rate of fiber extraction; R_0 is the radius of the semifinished product; T_t is the temperature at the boundaries of the theoretical region.

Let us illustrate the dependence of the profile of the stream R(x) and the distributions of velocity v(x) and temperature T(x) on different parameters of the extraction process. We assumed the following in the calculations: R_0 = 5 mm, fiber radius at the receiving unit 64 μm, glass density $\rho = 2.2 \cdot 10^3$ kg/m^3, specific heat of the glass $c = 1.043 \cdot 10^3$ J/(kg·K), σ = 0.3 N/m, the refractive index of the gas blown through the furnace n_c = 1, its specific heat $c_{p\ell} = 5.2 \cdot 10^3$ J/(kg·k), temperature at the inlet $T_{\ell 1}$ = 400°C, velocity v_ℓ = 1 m/sec, integral emittance of the surface of the furnace ε_f = 0.97. It was assumed that the form of the inside surface of the heating element was cylindrical and that the surface had a radius R_f = 10 mm. The temperature distribution along its surface was modeled by the function (see Fig. 1)

$$T_f(\theta) = \begin{cases} T_{f1}, & -a_1 < \theta < 0,\ (a_2 - a_1) < \theta < (l - a_1), \\ T_{f1} + (T_{f2} - T_{f1})\, 6.75 \dfrac{\theta^2(\theta_t - \theta)}{\theta_t^2}, & 0 \leqslant \theta \leqslant \frac{2}{3}\theta_t, \\ T_{f2}, & \frac{2}{3}\theta_t \leqslant \theta \leqslant \theta_0 - \frac{2}{3}\theta_t, \\ T_{f1} + (T_{f2} - T_{f1})\, 6.75 \dfrac{(\theta_0 - \theta)^2(\theta + \theta_t - \theta_0)}{\theta_t^2}, & \theta_0 - \frac{2}{3}\theta_t \leqslant \theta \leqslant \theta_0, \end{cases} \tag{1.6}$$

where $\theta_0 = a_2 - a_1$; $\theta = \eta - a_1$; T_{f2} is the maximum temperature of the surface of the heating element; $\theta_t/\theta_0 = \xi$, $0.75 \leqslant \xi \leqslant 0.075$. Equation (1.6) adequately approximates the temperature distribution along the surface of the heating element, since it presumes that the temperature profile includes a core θ_ξ with a constant temperature and a gradient part (near the boundary surfaces), where temperature changes in accordance with the law of a cubic parabola. Varying the temperatures T_{f1}, T_{f2} with the size of the central section (θ_ξ is determined by the constant ξ, $\theta_\xi = 0$ at $\xi = 0.75$ and $\theta_\xi = 0.9\theta_0$ at $\xi = 0.075$) and the length of the heated section $a_2 - a_1$ makes it possible to change the temperature distribution along the surface of the heating element and thereby model different thermal regimes for fiber extraction. The dependence of the viscosity of the glass melt on temperature was taken from [9], while the size of the heated section is always 10 cm.

Figures 2 and 3 show the form of the stream surface R(x) and the temperature distribution T(x) for the heated section for different withdrawal rates 2, 3 and different temperature

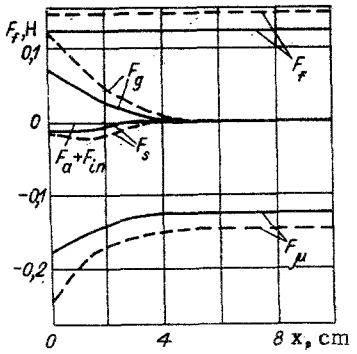

Fig. 5

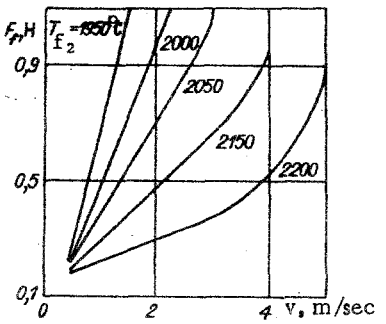

Fig. 6

profiles along the heating element 1, 4. Here, curves 2 and 3 correspond to the temperature distribution along the surface of the heating element, T_{f1} = 1400°C, T_{f2} = 2100°C, ξ = 0.375, extraction rate v_ℓ = 0.5 m/sec (for 3) and v_ℓ = 1.5 m/sec (for 2). Curves 1 and 4 correspond to v_ℓ = 0.5 m/sec, T_{f1} = 1200°C, T_{f2} = 2100°C, ξ = 0.75 (for 1) and ξ = 0.075 (for 4). It is evident that the temperature distribution and the configuration of the deformation region depend appreciably on the conditions of fiber formation and, in the present case, on the extraction rate and the thermal regime for heating the semifinished product in the furnace. The axial velocity changes fairly smoothly in the upper part of the deformation region. The main increase in axial velocity occurs on the final section of fiber formation over a very short time interval.

The length of the deformation region during heating of the semifinished product in the furnace (by the deformation region, we mean the region of the stream located between the sections where the stream is thinned and where its velocity changes from the rate of product feed into the heating zone to the extraction velocity, to within 1%) depends mainly on the diameter of the semifinished product, extraction rate, and the amount of heat supplied and its lengthwise distribution. The lengthwise distribution of heat flux is in turn determined by the form of the heating element and the temperature profile along its surface. The length of the deformation region also depends on the outgoing heat flux, which in turn depends on the coefficient of external heat transfer. Figure 4 shows the dependence of the length of the deformation region on v_ℓ ($R_0 = 0.5$cm, $\xi = 0.375$, $T_{f_1} = 1400$°C, $T_{f_2} = 2100$°C.

The calculated results show that, due to the large value of λ_{ef} (according to our estimates, $\lambda_{ef} \sim 40$ W/(m·K) [4]), ignoring the term $\frac{\partial}{\partial x}\left(\lambda_{ef} R^2 \frac{\partial T}{\partial x}\right)$, in the energy equation will lead to significant errors in the determination of the temperature field in the deformation region. At the same time, the amount of heat given off due to dissipation of mechanical energy does not significantly affect the temperature distribution.

2. In developing mathematical models of the drawing of optical fibers it is usually assumed that the viscous forces are so great that, compared to them, it is possible to ignore the force of gravity, friction against the air, surface tension, and inertia. However, this is not certain, since the effect of each component of stream tonsion F_f changes along the deformation region and depends on the specific conditions of fiber formation.

The equation expressing the balance of forces acting in the deformation region at a distance x along the region is written in the form [10]

$$F_f + F_g(x) = F_\mu(x) + F_s(x) + F_{in}(x) + F_a(x), \tag{2.1}$$

where $F_g(x)$, $F_\mu(x)$, $F_s(x)$, $F_{in}(x)$, $F_a(x)$ are the force of gravity, viscous drag, surface tension, inertia, and air resistance.

We will examine each component of stream tension F_f in Eq. (2.1) separately. The force F_μ depends on the velocity and viscosity of the glass in the given section. Assuming that we are dealing with the simple uniaxial tension of a Newtonian fluid

$$F_\mu = 3\pi\mu R^2 \partial v/\partial x. \tag{2.2}$$

Surface tension is manifest due to curvature of the stream surface and, in accordance with the Laplace law, is equal to

$$F_s = \pi R^2 \sigma H, \tag{2.3}$$

the force F_{in} is expended on acceleration of the fluid from a certain velocity in the section x to the fiber extraction velocity in the section $x = \ell$, i.e.

$$F_{in} = \pi\rho \int_x^l R^2 v \frac{\partial v}{\partial x} dx. \tag{2.4}$$

the last term in the right side of (2.1) is determined by frictional resistance during the motion of the stream in the environment

$$F_a = 2\pi \int_x^l P_{xr} R dx, \tag{2.5}$$

where P_{xr} is the local shear stress which develops on the surface of a body moving at the velocity v in a medium with the density ρ_g; $P_{xr} = (1/2) \times \rho_g \nu^2 \bar{c}_f$; $\bar{c}_f$ is the mean drag coefficient, dependent on the velocity of the body, the geometry of its surface, and the kinematic viscosity of the medium ν_g. The value of $\bar{c}_f$ can be evaluated from the formula $\bar{c}_f = 0.4(\mathrm{Re}_2)^{-0,7}$, which was obtained in [11] on the basis of the theory of a turbulent boundary layer for a stationary cylinder in a longitudinal gas flow. Here, $\mathrm{Re}_2 = v_g R/\nu_g$. In the region of formation of the optical fiber in the direction of the extraction force, the force of gravity acts on the stream

$$F_g = \pi\rho g \int_x^l R^2 dx. \tag{2.6}$$

The tension in any section of the stream can be assumed constant, while the relationship of the remaining forces with each other changes along the stream. Figure 5 shows the results of the use of Eqs. (2.2)-(2.6) to calculate individual components of the tension on the fiber along the formation zone (the solid lines correspond to $R_0 = 0.5$ cm, $v_l = 0.5$ m/sec, $T_{f1} = 1400$°C, $T_{f2} = 2050$°C, $\xi = 0.375$, while the dashed lines correspond to $R_0 = 0.9$ cm). Besides F_μ, F_g and F_s turn out to have a significant effect on fiber tension in the upper part of the deformation region. Farther along the path of deformation, F_f is almost completely balanced by viscous drag F_μ. The effect of the force of gravity and surface tension depend on the specific conditions of formation. Specifically, their effect depends on the method used to heat the semifinished product, since this for the most part determines the form of the deformation region [12]. It follows from (2.3) and (2.6) that we should expect the effect of F_s to increase with a decrease in the length of the deformation region, since in this case there will be an increase in the mean curvature of the surface H and a reduction in the effect of F_g. On the other hand, the level of the significance of F_g and F_s depends appreciably on the degree of heating of the glass along the deformation zone. For example, with $R_0 = 0.5$ cm, $v_l = 0.5$ m/sec, $T_{f1} = 1400$°C, $T_{f2} = 2000$°C, $\xi = 0.75$ the contribution of gravity and surface tension to the overall tension of the stream becomes small over the entire deformation region compared to the contribution of viscous drag. The small forces of inertia and air resistance – in contrast to the case of the formation of textile polymers and operational glass fibers [10, 13] – are attributable to the low extraction velocity. Thus, the completed calculations show that in developing mathematical models of the process of optical fiber drawing, it is best to consider F_g and F_s in the equation of motion along with F_μ.

3. An examination of the force balance equation (2.1) shows that the tensile force depends on the conditions of fiber formation and the properties of the glasses. Figure 6 shows the dependence of F_f on v_ℓ and the heating regimes in the furnace ($T_{f1} = 1400$°C, $\xi = 0.375$, $R_0 = 0.5$ cm). Calculations of both F_f and R indicate that the tensile force and the form of the stream surface (see Part 1) are very sensitive to fluctuations in the conditions of fiber formation (a change in the feed or extraction rates, cooling and heating conditions, the physical characteristics of the glasses) and can therefore be used as characteristics of the stability of the drawing operation. Deviations of these quantities from their nominal values can be used to construct algorithms for controlling the drawing process. On the other hand, during tension of the fibers a large role is played by the change in the viscosity of the glass along the deformation path. The viscosity in turn depends on several factors, the principal factor being temperature. The data presently available on μ is ill-suited for reliable use in specified applied investigations because the viscosity of the glass is very sensitive to processing features and chemical composition [9]. Equation (2.1), for a steady-

state stream of molten glass, is equivalent to motion equation (1.2); thus, with a known form of the stream surface R(x) and a known extraction force F_f – which can be determined experimentally – we determine the viscosity profile along the deformation region as:

$$\mu(x) = \frac{\frac{F_f}{\pi} + \rho g \int_x^l R^2 dx - R^2 \sigma H - \rho \int_x^l R^2 v \frac{dv}{dx} dx - 2 \int_x^l P_{x\tau} R dx}{3R^2 \frac{dv}{dx}}. \quad (3.1)$$

Equation (3.1) was obtained from (2.1) after inserting the components of stream tension, and it allows us to determine the temperature dependence of viscosity with simultaneous measurement of the form of the stream, extraction force, and the temperature distribution along the deformation region during fiber deformation. Equation (3.1) can also be used to find the temperature distribution by measuring R(x) and F_f if $\mu(T)$ is known for the glass.

LITERATURE CITED

1. T. J. Miller, "Use of heat-transfer analysis in the manufacture of large preform by the MCVD process," AIChE J., 80, No. 236 (1984).
2. V. N. Vasil'ev and G. N. Dul'nev, "Formulation of the problem of drawing optical fibers with shear flow," in: Energy Transfer in Convective Flows [in Russian], ITMO AN Belorussian SSR, Minsk (1985).
3. V. D. Naumchik, "Quasiunidimensional model of the drawing of optical fibers," loc. cit.
4. V. N. Vasil'ev, Ya. I. Lanin, and V. D. Naumchik, "Analysis of radiant heat transfer in the drawing of optical fibers," in: Mathematical Models of the Theory of Transport in Inhomogeneous and Nonlinear Media with Phase Transformations [in Russian], ITMO AN Belorussian SSR, Minsk (1986).
5. S. W. Churchill, "A comprehensive correlating equation for laminar, assisting, forced, and free convection," AIChE J., 23, No. 1 (1977).
6. O. G. Martynenko, and Ya. A. Sokovishin, Free-Convective Heat Transfer [in Russian], Nauka i Tekhnika, Minsk (1982).
7. V. P. Isachenko, V. A. Osipova, and A. S. Sukomel, Heat Transfer [in Russian], Énergoizdat, Moscow (1981).
8. V. G. Borovskii and V. A. Shelimanov, Heat Transfer of Small-Radius Cylindrical Bodies and Their Systems [in Russian], Naukova Dumka, Kiev (1985).
9. V. K. Leko, E. V. Meshcheryakova, et al., "Study of the viscosity of commercial quartz glasses," Opt. Mekh. Promst., No. 12 (1974).
10. G. Manfre, "Forces acting in continuous drawing of silica fibers," Glass Technol., 10, No. 4 (1969).
11. Glicksman, "Dynamics of a free preheated stream at low Reynolds numbers," Trans. ASME Ser. D, 90, No. 3 (1968).
12. S. M. Oh, "Cooling rates of optical fibers during drawing," Ceram. Bull., 58, No. 11 (1979).
13. A. Zyabitskii, Theoretical Principles of Fiber Formation [Russian translation], Khimiya, Moscow (1979).